Hydrological Cycles Change in the Yellow River Basin during the Last Half of the Twentieth Century

QIUHONG TANG

Institute of Industrial Science, University of Tokyo, Tokyo, Japan, and Department of Civil and Environmental Engineering, University of Washington, Seattle, Washington

TAIKAN OKI AND SHINJIRO KANAE

Institute of Industrial Science, University of Tokyo, Tokyo, Japan

HEPING HU

Institute of Hydrology and Water Resource, Tsinghua University, Beijing, China

(Manuscript received 22 January 2007, in final form 29 June 2007)

ABSTRACT

A distributed biosphere hydrological (DBH) model system was used to explore the internal relations among the climate system, human society, and the hydrological system in the Yellow River basin, and to interpret possible mechanisms for observed changes in Yellow River streamflow from 1960 to 2000. Several scenarios were evaluated to elucidate the hydrological response to climate system, land cover, and irrigation. The results show that climate change is the dominant cause of annual streamflow changes in the upper and middle reaches, but human activities dominate annual streamflow changes in the lower reaches of the Yellow River basin. The annual river discharge at the mouth is affected by climate change and by human activities in nearly equal proportion. The linear component of climate change contributes to the observed annual streamflow decrease, but changes in the climate temporal pattern have a larger impact on annual river discharge than does the linear component of climate change. Low flow is more significantly affected by irrigation withdrawals than by climate change. Reservoirs induce more diversions for irrigation, while at the same time the results demonstrate that the reservoirs may help to maintain environmental flows and counter what otherwise would be more serious reductions in low flows.

1. Introduction

The Yellow River originates in the northern foothills of the Tibetan Plateau and empties into the Bohai Bay (Fig. 1). The river length is 5500 km with a basin area of 752 000 km^2 (the watershed area is as large as 795 000 km^2 if the endoreic inner flow area is included). Most of the basin's area is arid or semiarid. The Yellow River is the main source of surface water in northwest and northern China. As of 1997 there were 107 million inhabitants and 12.6 million hectares of cultivated land in the watershed, representing 8.6% and 13.3% of the national totals, respectively (Yellow River Commission 1999).

As in many major rivers, including the Colorado, the Nile, and the Ganges, humanity has extensively altered the Yellow River system through diversions and impoundments (Vitousek et al. 1997). Since the completion of a large irrigation project in 1969, the lower Yellow River has increasingly suffered from extreme low-flow conditions, and parts of the lower reaches are now often dry. This phenomenon, that is, zero flow in sections of the river channel, has occurred more and more often during the last 30 yr. The duration of these episodes and the zero-flow distance from the river month increased rapidly in the 1990s. Moreover, the flow at the primary tributaries in the source region of the river also subsequently began to encounter zero-flow episodes in the 1990s (Liu and Zheng 2004). Be-

Corresponding author address: Qiuhong Tang, Department of Civil and Environmental Engineering, University of Washington, Seattle, WA 98195-2700.
E-mail: qiuhong@hydro.washington.edu

DOI: 10.1175/2007JCLI1854.1

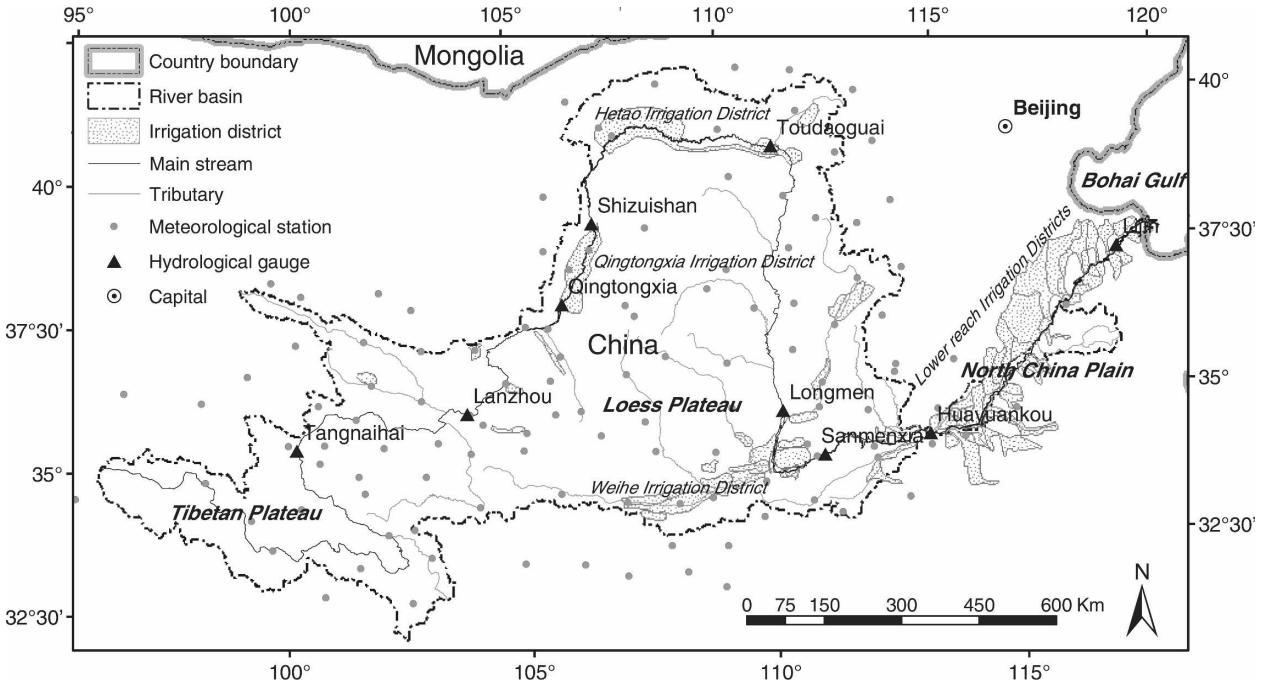

FIG. 1. The Yellow River basin.

cause of the social and environmental consequences, the drying of the Yellow River has attracted a good deal of research attention. Oki and Kanae (2006) argue that in the era of the "Anthropocene," where human impacts on natural processes are large and widespread, it no longer makes sense to study natural hydrological cycles in isolation. In this paper, we report the results of a study of the Yellow River that evaluates the separate and combined effects of climate change and human activities on the drying of the Yellow River.

Many studies of the Yellow River have analyzed monthly or annual streamflow observations for purposes of inferring statistical relationships between streamflow and climate, and/or have evaluated the implications of human activities on streamflow. Fu et al. (2004) analyzed hydroclimatic trends at 44 meteorological stations and 3 hydrologic gauges in the river basin from the 1950s to the 1990s. They found that trends in precipitation were generally not significant while natural runoff has decreased. Yang et al. (2004a) used meteorological data from 108 stations together with irrigation data and river discharge to investigate the reason for zero-discharge episodes. They found that the annual precipitation generally decreased while the air temperature generally increased. Xia et al. (2004) analyzed the river channel water balance of the upper, middle, and lower reaches and carried out a renewability index of water resources. Their analysis showed that the index had a significant declining trend from the 1950s through the 1990s, with the lowest index in the reach that is farthest downstream. Xu (2005a) proposed a quantitative index of river flow renewability and discussed the factors that influenced the index in the middle reaches of the basin. He found that the annual natural river flow, the runoff without anthropogenic effects, decreased in the last half century. Liu and Zheng (2004) detected hydrological trends by analyzing monthly precipitation from 44 meteorological stations and river discharge from two hydrological stations between 1952 and 1997. Their results suggested that increasing water resources development and utilization is the most important factor in causing the frequent zero-discharge episodes in the main stem in the lower basin. Xu (2005b) investigated changes in Yellow River discharge at its mouth. Their results showed that the contribution of increased water diversions to changes in annual water flux to the sea is 41.3%, precipitation changes account for 40.8%, temperature changes account for 11.4%, and erosion and sediment control measures account for 6.5%. Liu et al. (2003) estimated water replacement time for several river sections in the middle and the lower reaches. They found the renewal time was shortest during the May–October period, and annual renewal time tended to decrease from the middle to lower reaches. Huang and Zhang (2004) investigated hydrological responses to soil conservation practices in a tributary catchment. They found a clear decreasing trend in annual surface runoff and baseflow

volume that were attributable to conservation measures.

Several studies have been performed to investigate the effects of land use/land cover change on streamflow dynamics in the Yellow River basin. Wang et al. (2001) found the eco-environment in the source region of the Yellow River degraded markedly from the 1980s to the 1990s compared with the satellite images and field investigation results in the 1970s. Feng et al. (2005) classified and evaluated land degradation effects in the source region. Sun et al. (2001) analyzed statistical relationships between interannual change of fractional vegetation cover change and rainfall using a satellite [National Oceanic and Atmospheric Administration (NOAA) normalized difference vegetation index (NDVI) Pathfinder dataset]. They found that rainfall in the flood season is correlated with vegetation cover change in the grassland area. Yang et al. (2002) evaluated vegetation changes in the basin from 1982 to 1999 and found that vegetation cover on average had increased.

Some research has analyzed the human and natural factors responsible for Yellow River zero-discharge episodes and suggests ways of mitigating the phenomenon. Liu and Zhang (2002) analyzed hydroclimatic data related to human activities. Liu and Zhang (2004) analyzed the statistical relationship among observed annual rainfall, runoff, and water withdrawals and evaluated the relative contribution of climate change and human activities to main stem low-flow reductions. They found that climate change was responsible for about 75% of the changes in the upper reaches, and 43% in the middle reaches, with the balance attributable to human activities. In contrast, Chen and Mu (2000) concluded that water diversions are the major reason for zero-discharge episodes in the middle and lower reaches.

Although many studies have analyzed statistical relationships among hydroclimatic observations in the Yellow River basin, fewer have assessed the physical water cycle processes as they have been affected by climate change, water management, and land cover and land use change. Yang et al. (2004b) applied a semidistributed hydrologic model to the Yellow River basin. Evapotranspiration was simulated empirically, and energy fluxes and the effects of human activity were not taken into account. Mo et al. (2004) applied a process-based distributed model to simulate the temporal and spatial variations in evapotranspiration in a tributary basin. They used a soil–vegetation–atmosphere transfer (SVAT) scheme, which represented the coupled energy and water fluxes and compared model-estimated evapotranspiration with observed precipitation minus discharge at the outlet. However, their model did not consider the effects of topography and river routing. Other studies, such as Russell and Miller (1990), Oki et al. (1999), and Nijssen et al. (2001), have used macroscale hydrological models (MHMs), which are closely related to SVATs, by also representing the effects of river routing, to link climate predictions from global atmospheric models to water resource systems at the river basin scale on large spatial scales and long time scales. Hirabayashi et al. (2005) performed a 100-yr global retrospective estimation of the terrestrial water cycle with an MHM. While MHMs, like SVATs, are usually based on physical principles and therefore have the potential to help diagnose effects of anthropogenic change on river discharge and other aspects of the land surface hydrological cycle, most MHMs do not consider the effects of human activities (such as irrigation and dams), and the spatial resolution often is too coarse for water management purpose. An exception is the work of Haddeland et al. (2006a,b), who have incorporated within the variable infiltration capacity (VIC) MHM representations of irrigation and dams and evaluated them.

At much smaller scales, many hydrological studies have focused on the local scale of catchments or basins at which water management is effected. While MHMs often operate at coarse spatial resolution, some of them have increased in scale and geographical features to meet the interests of human society (Decharme and Douville 2006; Sheffield et al. 2004). The coupled vertical and lateral water fluxes simulation at relatively fine spatial resolution (e.g., about 10-km grid cells) would help to represent the connections among hydrological components and the features of hydrosphere in which human society is often most interested. To describe the dynamic mechanisms of the water cycle, study of the SVAT, runoff generating, and river routing processes at large river basin scales is urgently needed. The coupled study of more sophisticated energy and water transfer processes, such as photosynthesis–conductance processes, which control the simultaneous transfer of CO_2 and water vapor into and out of leaves, will improve the understanding of the physical mechanisms between climate change, vegetation change, human activities, and the hydrological pattern in the continental-scale river basin. That will give a scientific basis for interpreting the Yellow River zero-discharge phenomena.

In this study, we used a distributed hydrological model that couples a SVAT scheme to represent land–atmosphere interactions and the effects of land cover

and land use change, a physically based MHM that represents runoff generation processes as they are affected (both directly and indirectly) by land cover and land use change, and the effects of human activities on the land surface water budget into one comprehensive hydrological model system. We then apply the model to analyze the physical connections among climate, vegetation changes, and water management in the Yellow River basin. First, we briefly describe the distributed biosphere hydrological (DBH) modeling system and the data used in our model simulations. Then, we describe the approach to representing physical connections between climate, vegetation condition change, and human manipulation of the water cycle. Finally, we use the model to assess the relative contributions of changes in climate, vegetation, and water management as they are related to Yellow River zero-discharge episodes.

2. Data and methodology

a. Data analysis

Hydroclimatic data from 120 meteorological stations inside and close to the Yellow River basin were obtained from the China Meteorological Administration (CMA) and the Hydrological Bureau of the Ministry of Water Resources of China (Ministry of Water Resources 1991). The dataset includes daily precipitation; daily mean, maximum, and minimum temperatures; mean surface relative humidity; sunshine duration; cloud amount; and river discharge from 1950 to 2000. Several stations on the Qinghai–Tibet Plateau were established at the end of the 1950s, which dictated the study period from 1960 to 2000 (Liu and Chen 2000; Tang et al. 2007b). Biophysical data, specifically the leaf area index (LAI) and the fraction of photosynthetically active radiation absorbed by the green vegetation canopy (FPAR) were obtained from Myneni et al. (1997). The LAI dataset is available with monthly temporal frequency and 16 km $\times$ 16 km spatial resolution from 1982 to 2000. Vegetation change information was analyzed in Tang et al. (2007b), as was information about changes in hydroclimatic conditions. The LAI values show an obvious increasing trend, most likely because of increased irrigated area. On the other hand, precipitation decreased in the Loess Plateau, which implies that the reductions of discharge in the upper and middle reaches are due, at least in part, to less precipitation.

b. Methodology

The DBH model is described in detail in Tang (2006), and we summarize only the key aspects here. DBH embeds a biosphere model into a distributed hydrological scheme, which represents the effects of topography on runoff generation and the effects of vegetation on surface turbulent energy fluxes at a continental river basin scale (Tang et al. 2006). DBH incorporates recent multidisciplinary developments, which results in a noticeable improvement in hydrological simulation. These geophysical advances include the new insights into heat flux in the SVAT processes by meteorologists, more realistic models to describe the photosynthesis–conductance process, progress in extracting reliable land surface information from remote sensing data, and development of geographic information system (GIS) techniques to extract topographic variables from digital elevation models (DEMs).

In the DBH model system, satellite data are used to describe the vegetation phenology. Time series fields of FPAR and LAI data were derived from the Advanced Very High Resolution Radiometer (AVHRR) sensor on the NOAA series of meteorological satellites. FPAR is used directly in the photosynthesis–conductance calculation, while LAI is used in the specification of land surface turbulent transfer and reflectance properties. The Food and Agriculture Organization (FAO) Digital Soil Map of the World (FAO 1995) was used to produce gridded soil properties, such as the soil water potential at saturation ψ_s (m), soil hydraulic conductivity at saturation K_s (m s^{-1}), soil wetness parameter b, and porosity θ_s (Cosby et al. 1984). Meteorological data from ground stations was gridded into 10-km grid cells using the angular distance weighted (ADW) method (Tang 2006). Because the revised Simple Biosphere Model (SiB2) needs subdaily atmospheric forcing, the gridded meteorological data were downscaled to hourly. The hourly mean temperature was estimated from the daily maximum and minimum temperatures using an empirical model (TM) developed by Cesaraccio et al. (2001). We adopted a new and widely validated radiation model (Yang et al. 2001; Yang and Koike 2005) to estimate the radiation, with hourly sunshine data interpolated from daily data following Revfeim (1997). The downward longwave radiation flux was calculated following Jiménez et al. (1987). The gridded data were used to drive SiB2 (Sellers et al. 1996) and calculate the transfer of energy, mass, and momentum between the atmosphere and the surface of the earth. The DBH model was therefore run at 10 km $\times$ 10 km spatial resolution.

A groundwater reservoir was added to the SiB2 3-layer isothermal model to calculate hydraulic diffusion and gravitational drainage of water in the soil

(Tang 2006). The equation used to describe vertical exchanges between soil layers is

$$Q = K\left(\frac{\partial\psi}{\partial z} + 1\right), \tag{1}$$

where Q is vertical water exchange between soil layers (m s^{-1}), K is estimated effective hydraulic conductivity between soil layers (m s^{-1}), ψ soil moisture potential (m), and z is vertical distance. The transfer of water between groundwater and soil water is given by

$$Q_{3g} = K_{3g}\left(\frac{\partial\psi_{3g}}{\partial z_{3g}} + 1\right), \tag{2}$$

where Q_{3g} is the vertical water exchange between soil recharge zone (the third soil layer) and groundwater layer (m s^{-1}), K_{3g} is the estimated effective hydraulic conductivity between soil layer and groundwater layer (m s^{-1}), ψ_{3g} is the soil moisture potential (m), and z_{3g} is the vertical distance. The soil moisture potential ψ_3 of the soil recharge zone is taken from the empirical relationship of Clapp and Hornberger (1978):

$$\psi_3 = \psi_s W_3^{-b}, \tag{3}$$

where W_3 is the soil moisture wetness fraction in the soil recharge zone, equal to the ratio of volumetric soil moisture to saturation soil moisture. The soil hydraulic conductivity of the soil recharge zone K_3 is obtained from the saturation hydraulic conductivity K_s (Clapp and Hornberger 1978):

$$K_3 = K_s\left(\frac{\psi_s}{\psi_3}\right)^{(2b+3)/b} = K_s W_3^{(2b+3)}. \tag{4}$$

The effective hydraulic conductivity K_{3g} then is estimated as

$$K_{3g} = f_{ice}\left(\frac{K_3\psi_3 - K_s\psi_s}{\psi_s - \psi_3}\right)\left(\frac{b}{b+3}\right), \tag{5}$$

where the soil freeze factor f_{ice} is a function of temperature defined in SiB2 (Sellers et al. 1996).

The flow between the river network and the groundwater is considered to be groundwater flow to a ditch over a sloping impermeable bed (Childs 1971; Towner 1975). This conceptual representation of river–groundwater exchange is shown in Fig. 2. Assuming that the flow lines are approximately parallel to the bed, according to the Dupuit–Forchheimer approximation, the flow of water per unit width of the river can be written

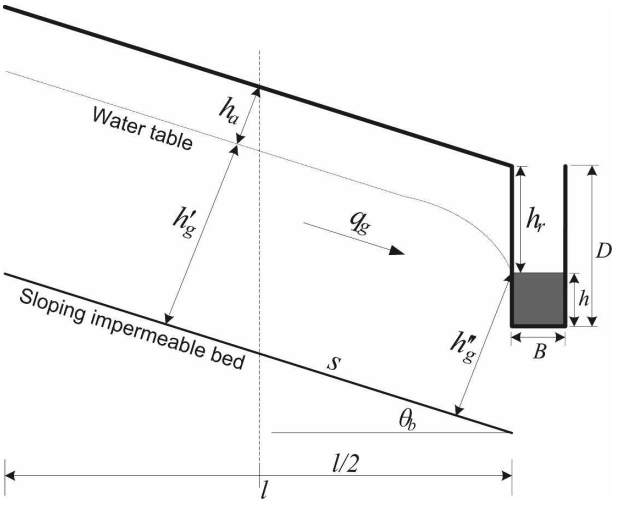

FIG. 2. Conceptual representation of river–groundwater exchange.

in terms of the hydraulic conductivity and the absolute slope of the water table:

$$q_g = K_s\frac{h'_g + h''_g}{2}\left[\frac{h'_g - h''_g}{l/(2\cos\theta_b) + h_r\sin\theta_b}\cos\theta_b + \sin\theta_b\right], \tag{6}$$

where h'_g is the averaged aquifer thickness; $h''_g = h_a + h'_g - h_r\cos\theta_b$ is the aquifer thickness at the river; and l is the width of hillslope, which is set as half of the value of the grid area to river length in the grid cell. The groundwater depth change is then estimated from the water reservoir storage change. The surface overland flow and river flow are described by the kinematic wave model (Lighthill and Whitham 1955; Chow 1959).

An irrigation scheme is incorporated in the DBH model to estimate human effects on the hydrological cycle using the Global Map of Irrigated Areas (Tang et al. 2006; Siebert et al. 2005). In each grid cell, land use was partitioned into an irrigated and unirrigated fraction. The irrigated part was set to SiB2 land cover type "Agriculture or C3 Grassland." The unirrigated part was obtained from the Global Land Cover Characterization dataset (Loveland et al. 2000). The irrigation scheme was based on SiB2 simulated soil moisture in the irrigated tiles and available water for irrigation. The irrigation started when the soil moisture was below the wilting point level and continued until soil moisture reached field capacity level. The irrigation approach is similar to Haddeland et al. (2006a). However, the irrigation scheme is coupled online in the DBH model. Crop evapotranspiration is estimated from satellite-observed vegetation data within the framework of the SVAT scheme. The available water for irrigation was

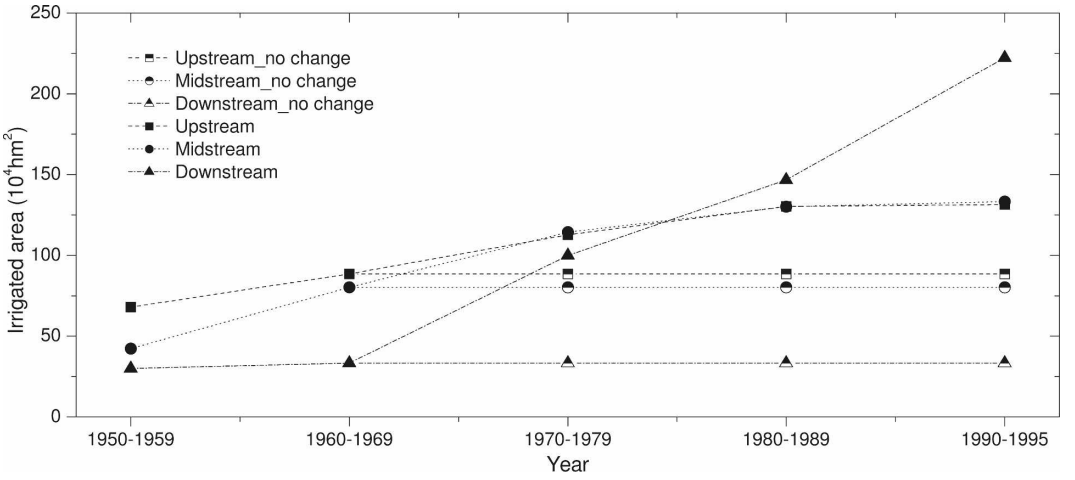

FIG. 3. The irrigated area in the Yellow River basin.

estimated based on the predicted river flow by the river routing module. Irrigation water can be extracted from two possible sources: local river runoff or river runoff at an assigned river channel (usually a main stem river reach). In most cases, irrigation water was assumed to be extracted from river runoff locally, which appears to be the case in practice (irrigation districts usually extract irrigation water from specific river channels). The irrigation water transportation loss, the most important factor that may affects actual irrigation water withdrawals from river, was considered with a simple water balance method for the irrigated and unirrigated part of each grid cell (Tang et al. 2007a).

A control (hydrology) run was performed by driving the DBH model with observed climate data for the period 1960–2000. Vegetation parameters prior to the 1980s are unavailable from satellite data, and therefore linear trends for the post-1980 period were extrapolated back to 1960. The baseline irrigated area was taken from the Global Map of Irrigated Areas (Tang et al. 2007c; Siebert et al. 2005) for the 1990s, and was adjusted to conditions from the 1960s on based on Liu and Zhang (2002), Yang et al. (2004a), and Xia et al. (2004). The spatial distribution of irrigated area was estimated from the Global Map of Irrigated Areas using the geometric proportion scale method (Haddeland et al. 2006a). Figure 3 shows the estimated history of irrigated area changes in the Yellow River basin over the study period.

A set of scenarios was defined to prescribe the range of conditions that formed the basis for assessment of the relative effects of climate, vegetation change, and human activity on Yellow River zero-discharge episodes during the period 1960–2000. The DBH model, using climate, vegetation, and irrigated area histories (all of which have changed substantially over the study period in various parts of the basin), was used to construct hydrologic conditions associated with each of the scenarios. The scenarios are S1: the control simulation with observed changes in climate, vegetation, and irrigated area over the study period; S2: the same forcing data as the control simulation except that the linear trend in climate data (i.e., precipitation, temperature, sunshine duration, and relative humidity) is removed and the mean values of the climate forcings are fixed to the means of the 1960s; S3: the same forcing data as the control simulation except that linear changes in vegetation data were removed and the mean was fixed at the level of the 1960s; S4: the same forcing data as the control simulation except that the irrigated area was fixed at the 1960s level; S5: a simulation where the linear trend in climate was removed as in S2, vegetation data were as in S3, and irrigated area data were as in S4; and S6: a stable simulation where climate conditions in the 1970s, 1980s, and 1990s repeated the climate conditions in the 1960s, with no vegetation or irrigated area changes (both fixed to the 1960s conditions).

Scenarios S2 (linear climate trends removed), S3 (no vegetation change), and S4 (no irrigation change) were designed to investigate the relative effects of each of the three change instruments on the hydrological cycle of the Yellow River basin individually. After gridding of the climate data used to force DBH, linear trends were fit to the daily climate forcings at each grid cell (Tang 2006). The areal climate data before and after removing tendency are shown in Fig. 4. Climate conditions in the 1960s were used as the reference condition; that is, the mean value was for the 1960s. The irrigated area in the 1960s was used as the reference value for

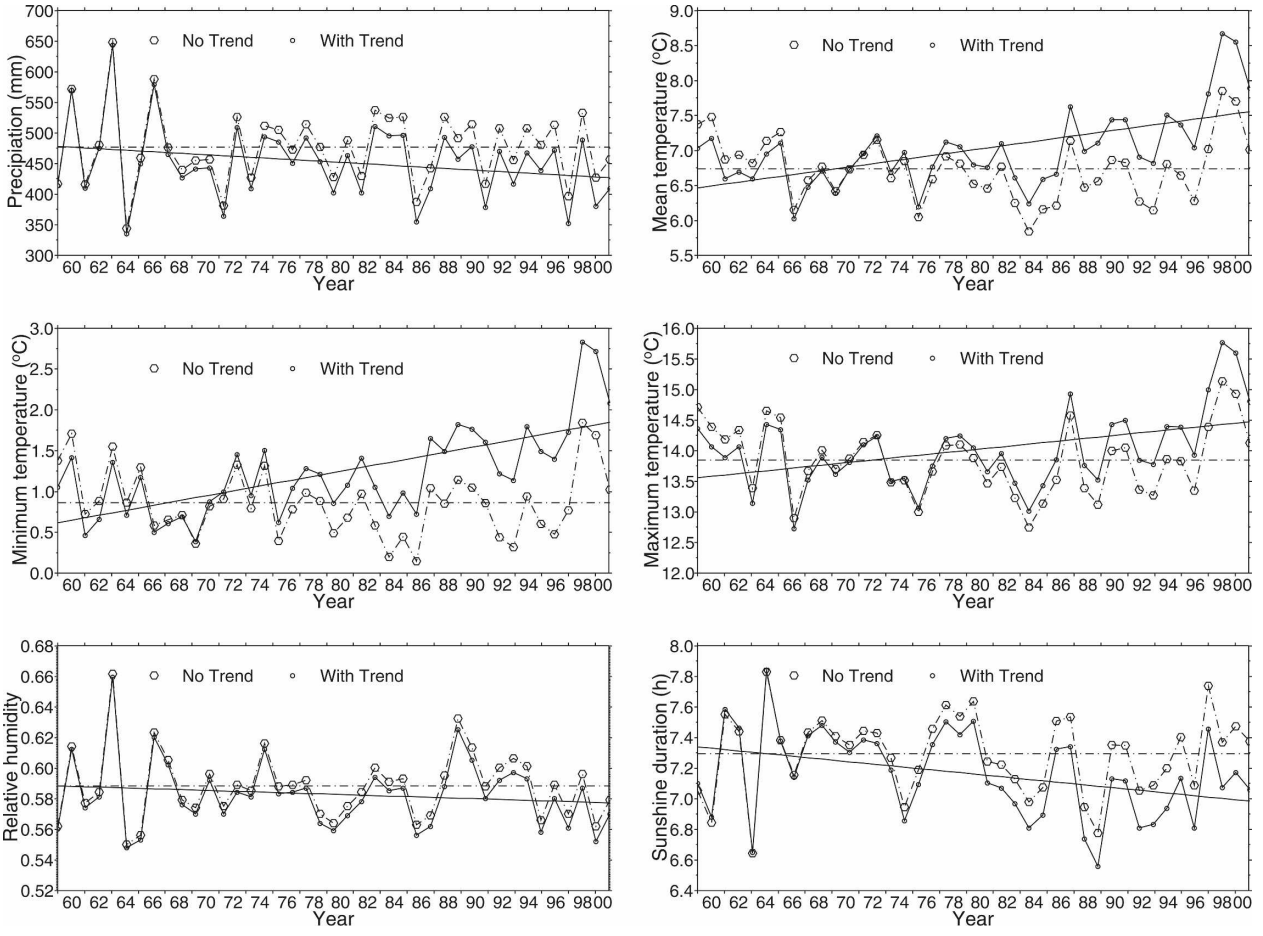

FIG. 4. Climate data with and without linear tendency.

scenario S2 (no irrigation change; Fig. 3). Vegetation data (LAI and FPAR) are available only from the early 1980s on. Therefore, the monthly data pattern was retained and the annual mean value was linearly extended back to the 1960s (see Fig. 5). Although a sophisticated method may help to reconstruct the historical vegetation data before the 1980s, the main purpose of this study is not to retrieve the vegetation data, but to demonstrate a scenario of vegetation change effect on hydrological cycles. The linear extension provided a simple possible way to drive the scenario. Based on the simulated results, the linear regression model was used to analyze the trend magnitude of simulated hydrological components. The effects of climate, vegetation, irrigation, and all changes combined were then estimated from the trend magnitude. The forcing data of both S5

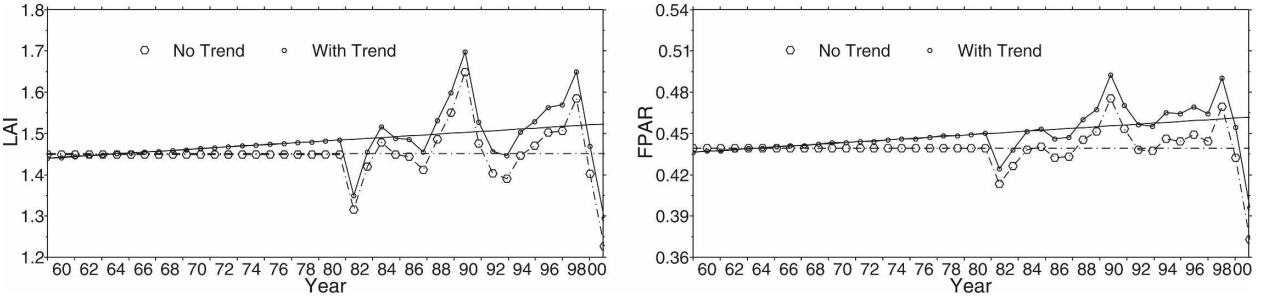

FIG. 5. Vegetation data extension and the data with and without linear tendency.

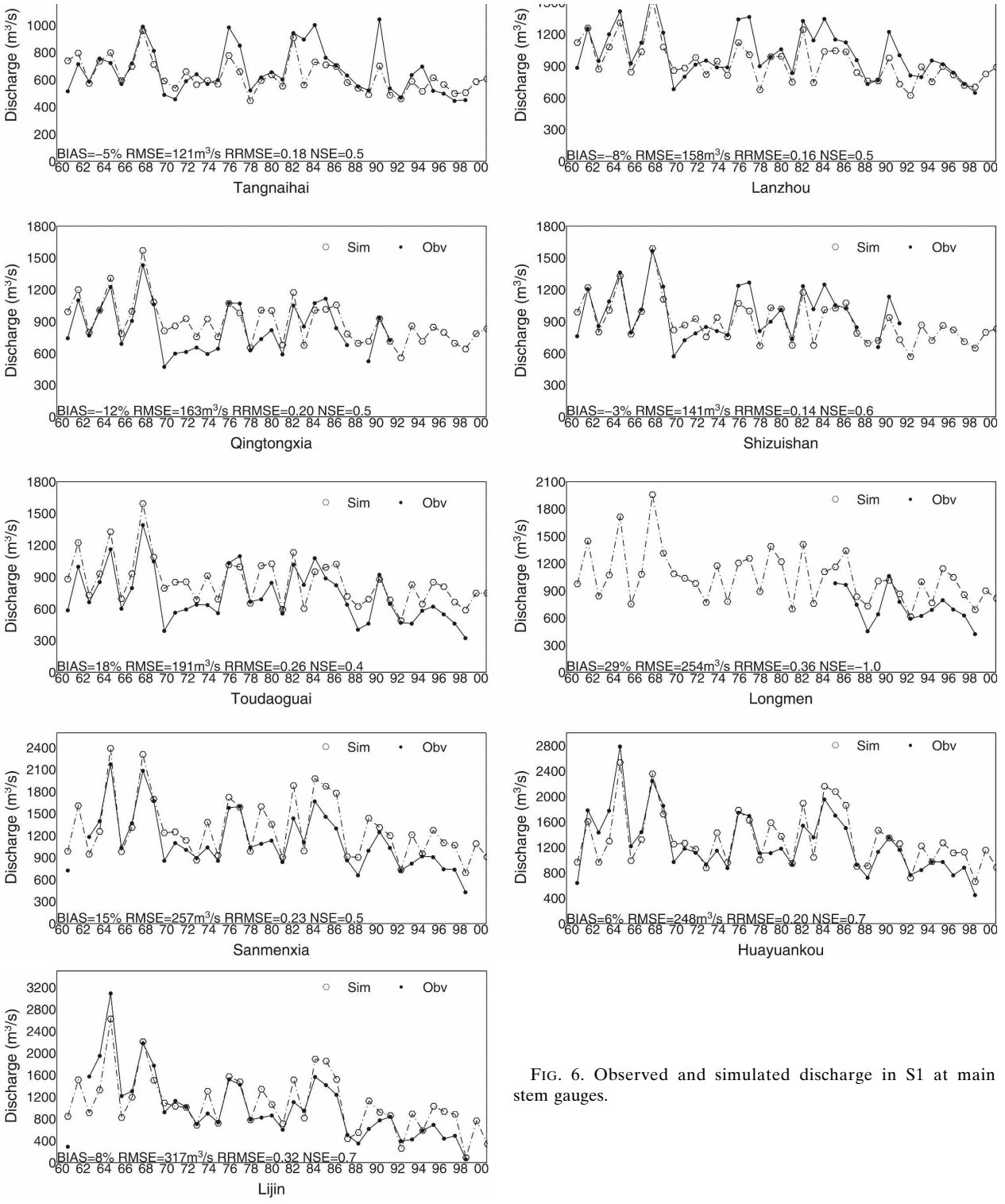

FIG. 6. Observed and simulated discharge in S1 at main stem gauges.

and S6 have no linear trend and were fixed to the 1960s conditions. However the climate temporal patterns in the 1970s, 1980s, and 1990s were fixed to the 1960s conditions in S6 and kept as the observations in S5. The difference between S5 and S6 (S6 − S5) was used to estimate the change magnitude of the simulated hydrological components caused by the climate temporal pattern.

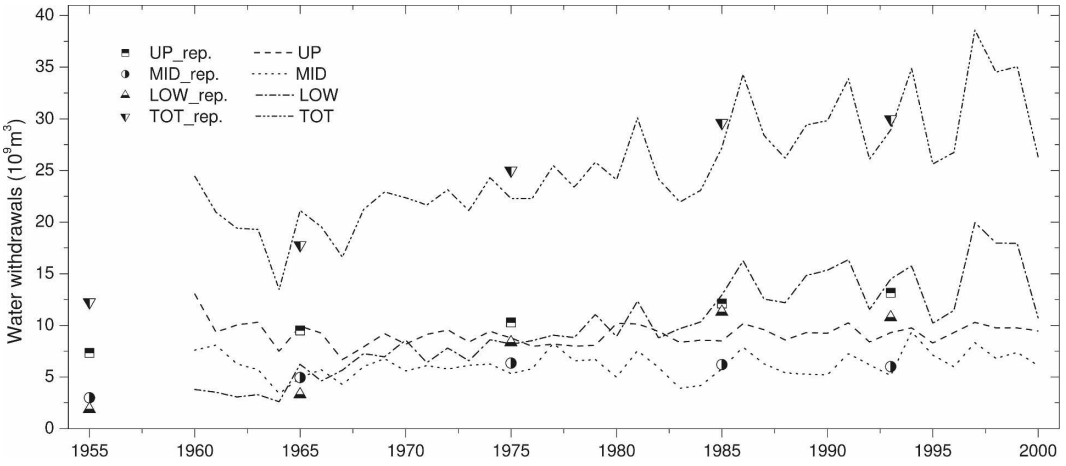

FIG. 7. Reported and simulated water withdrawals in S1 at the upper, middle, and lower reaches of the Yellow River.

3. Results and analysis

a. Control simulation

Figure 6 shows the observed and simulated discharge for S1 for main stem gauges from 1960 to 2000. The relative bias (BIAS), root-mean-square error (RMSE), relative root-mean-square error (RRMSE), and Nash–Sutcliffe efficiency coefficient (NSE; Nash and Sutcliffe 1970) are given in the figure. For most of the gauges, the simulated and observed discharge agree quite well, with BIAS less than 10% and NSE larger than 0.5 for the annual flows. And most of the observed trends are captured. The annual river discharges show large decreasing trends, especially at the lower reach gauges such as Sanmenxia, Huanyuankou, and Lijin. A sharp decrease is observed at the Lijin gauge, implying substantial diversions and consumptive use between the Huanyuankou and Lijin gauges.

The reported and simulated water withdrawals in S1, the control simulation from 1960 to 2000 at the upper, middle, and lower reaches of the Yellow River are shown in Fig. 7. The water withdrawals are satisfactorily reproduced by the control simulation. The simulated water withdrawals give a slight decrease for the upper reaches, while the reported values show a gradual increase. The discrepancy may be caused by various factors including irrigation water transportation loss, groundwater uptake, and various human decisions on agricultural practices, which are not explicitly modeled or well represented because of a lack of local information. Both reported and simulated water withdrawals show that changes in water withdrawals in the upper and middle reaches during the study period were small. Water withdrawals in the lower reaches increase by a factor of nearly 5 from the 1960s to the 1990s. This suggests that the lower reach water withdrawals have a much larger effect on hydrological changes in the Yellow River than do those in the upper and middle reaches.

Figure 8 shows predicted runoff, evapotranspiration, water withdrawals, and ground surface temperature changes in the subbasins of the Yellow River from 1960 to 2000 for the control simulation S1. Runoff decreases over most part of the river basin. Large runoff decreases are predicted (and observed) for the Loess Plateau, corresponding to precipitation decreases in that region. The simulated evapotranspiration also decreases over the Loess Plateau. The decrease in evapotranspiration is of the same order as the runoff decrease. Increased evapotranspiration was predicted for the Qingtongxia-Hetao irrigation district, the middle reach irrigation districts, and the lower reach irrigation districts. The large evapotranspiration in the lower irrigation districts indicates that human activities have affected the hydrologic cycle in that region. Water withdrawals increase over most of the basin. The largest increase of water withdrawals also occurs in the lower reaches. The ground surface temperature increases over the upper and middle reaches. The ground surface temperature increase over the Tibetan Plateau and Qingtongxia-Hetao district is related primarily to the observed air temperature increase. Increasing ground surface temperatures are also predicted over the Loess Plateau, which are in part a result of decreased precipitation and hence reduced evaporative cooling of the land surface. Small increases in air temperature are detected in the lower reaches and part of the middle reaches, but the simulated ground surface temperatures are decreasing. One reason may be that the large water withdrawals have increased evaporation and hence

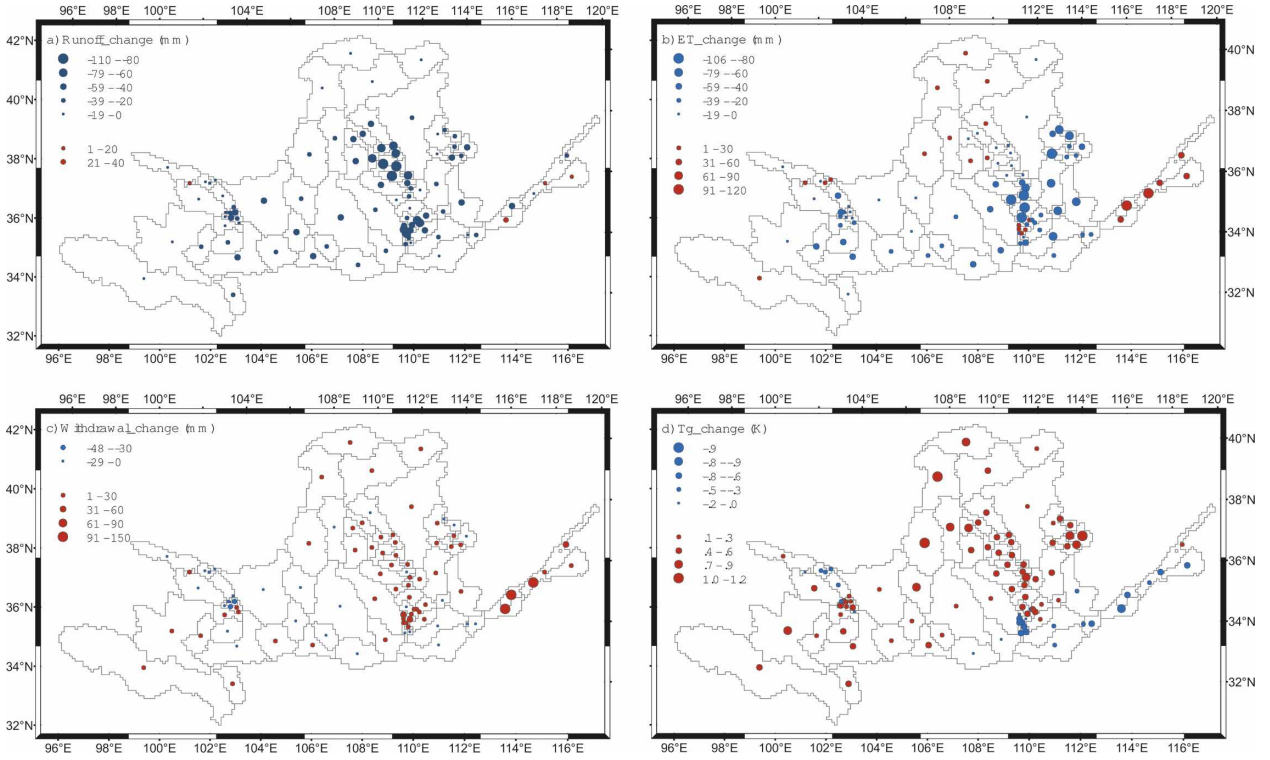

FIG. 8. Simulated changes from 1960 to 2000 in S1: (a) runoff change, (b) evapotranspiration change, (c) water withdrawals change, and (d) ground surface temperature change.

cooled the ground in the low reaches. Tang et al. (2007c) analyzed the effects of irrigation water withdrawals on ground temperature in the Yellow River. They found that latent flux increased and sensible flux decreased because of large irrigation water withdrawals. The possible contributions of these changes are analyzed below through assessment of the five scenarios.

The simulated sensible heating and canopy CO_2 assimilation fluxes are shown in Fig. 9. Decreases in sensible heating are predicted for the Qingtongxia-Hetao irrigation district, the middle reach irrigation districts, and lower reach irrigation districts. Large sensible heat flux decreases are also predicted for the lower reach irrigation districts, confirming that the large water withdrawals cool the ground in the lower reaches. The canopy CO_2 assimilation rate decreases in the subbasins without irrigation districts. The canopy CO_2 assimilation rate increases in the subbasins with large irrigation districts such as Qingtongxia-Hetao, the middle reach irrigation districts, and lower reach irrigation districts. The canopy CO_2 assimilation rate

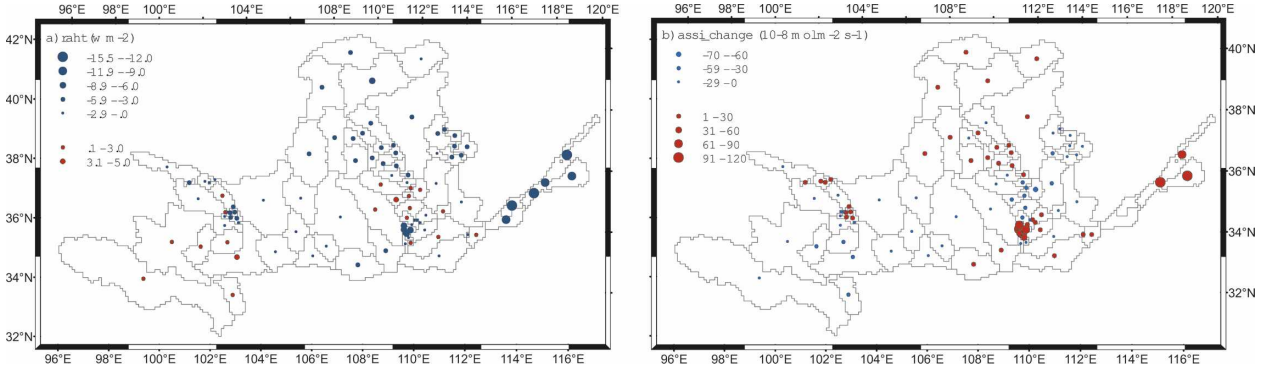

FIG. 9. Simulated (a) sensible heating (W s^{-2}) and (b) canopy CO_2 assimilation flux (10^{-8} mol m^{-2} s^{-1}) changes from 1960 to 2000 in S1.

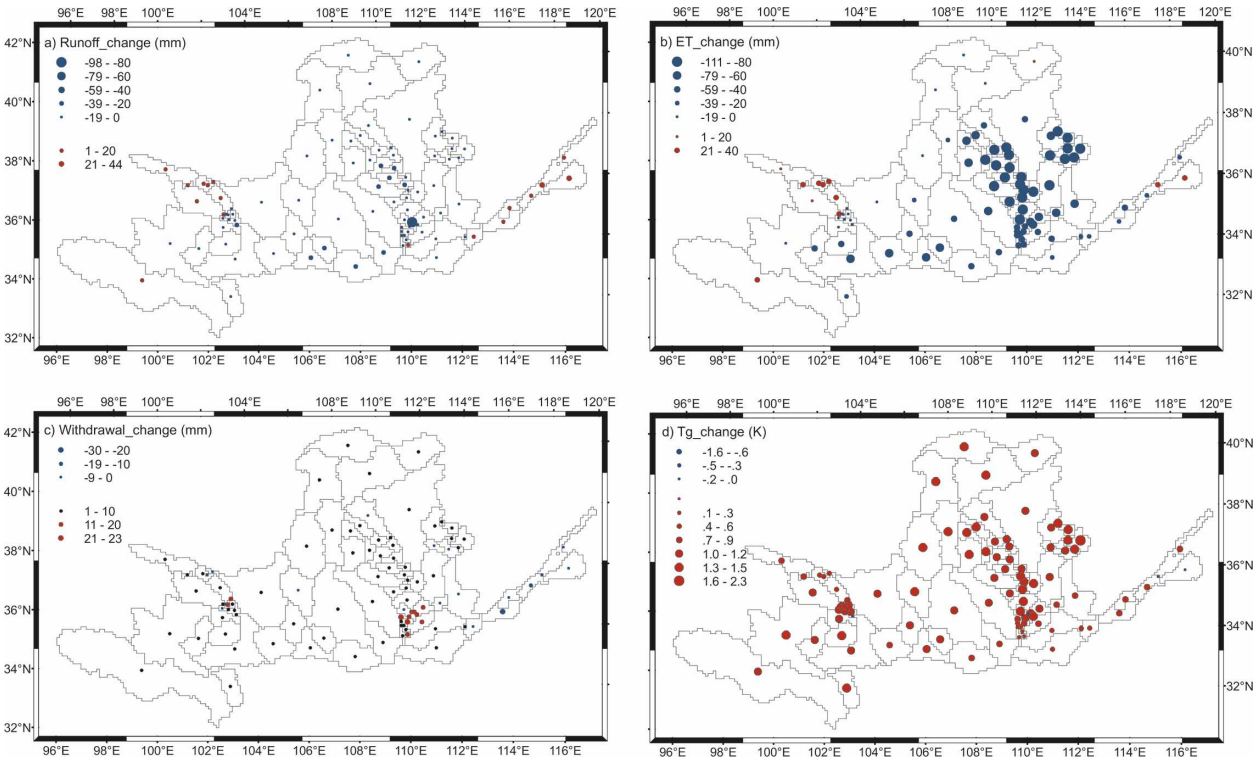

FIG. 10. Simulated changes contributed from climate linear change: (a) runoff change, (b) evapotranspiration change, (c) water withdrawals change, and (d) ground surface temperature change.

changes might be caused by the irrigation and vegetation recovery in irrigation districts and vegetation degradation elsewhere. In any event, the results suggest that human activity is altering the CO_2 assimilation pattern of the Yellow River basin.

b. Spatial changes of hydrology cycles

Figure 10, which shows simulated differences between S2 and S1 scenarios, illustrates the climate change (linear trend) on selected hydrological variables in the Yellow River basin from 1960 to 2000. Runoff decreases over most of the river basin as a result of precipitation decreases, which agrees with the data analysis results in Tang et al. (2007b). Large runoff decreases occur over the Loess Plateau. Runoff increases in the lower reaches, due to increased precipitation in the North China Plain. As a result of decreasing precipitation, evapotranspiration decreases over most part of the river basin. Extensive evapotranspiration decreases occur over the Loess Plateau, indicating that less precipitation increases the soil moisture stress and decreases the evaporation. Higher temperature may increase the evaporative demand; however, no significant tendency is detected over the Loess Plateau with the evaporative demand of the atmosphere as described in the data analysis paper Tang et al. (2007b). Because of less precipitation, water withdrawals from the river channel increase in the subbasins with irrigation districts over the Loess Plateau. Water withdrawals decrease a little in the North China Plain because of climate change, confirming that the climate becomes wet in that region. Ground surface temperature increases with climate change. The ground surface temperature change tendency is consistent with the observed air temperature increase over the entire river basin.

Figure 11 shows the contribution of vegetation change to the alteration of the hydrological components in the Yellow River basin from 1960 to 2000, which is represented by the simulated differences between scenarios S3 and S1. Runoff decreases slightly over most parts of the river basin. The runoff decrease is consistent with vegetation condition recovery (increased LAI) over the whole basin. Larger runoff decreases occur in irrigated areas, such as the lower reach irrigation districts, than in unirrigated areas. Evapotranspiration generally increases with increased LAI (much of which is associated with irrigation). The largest increases in water withdrawals occur in the lower reach irrigation districts, indicating more irrigation water is demanded to maintain soil moisture level in the

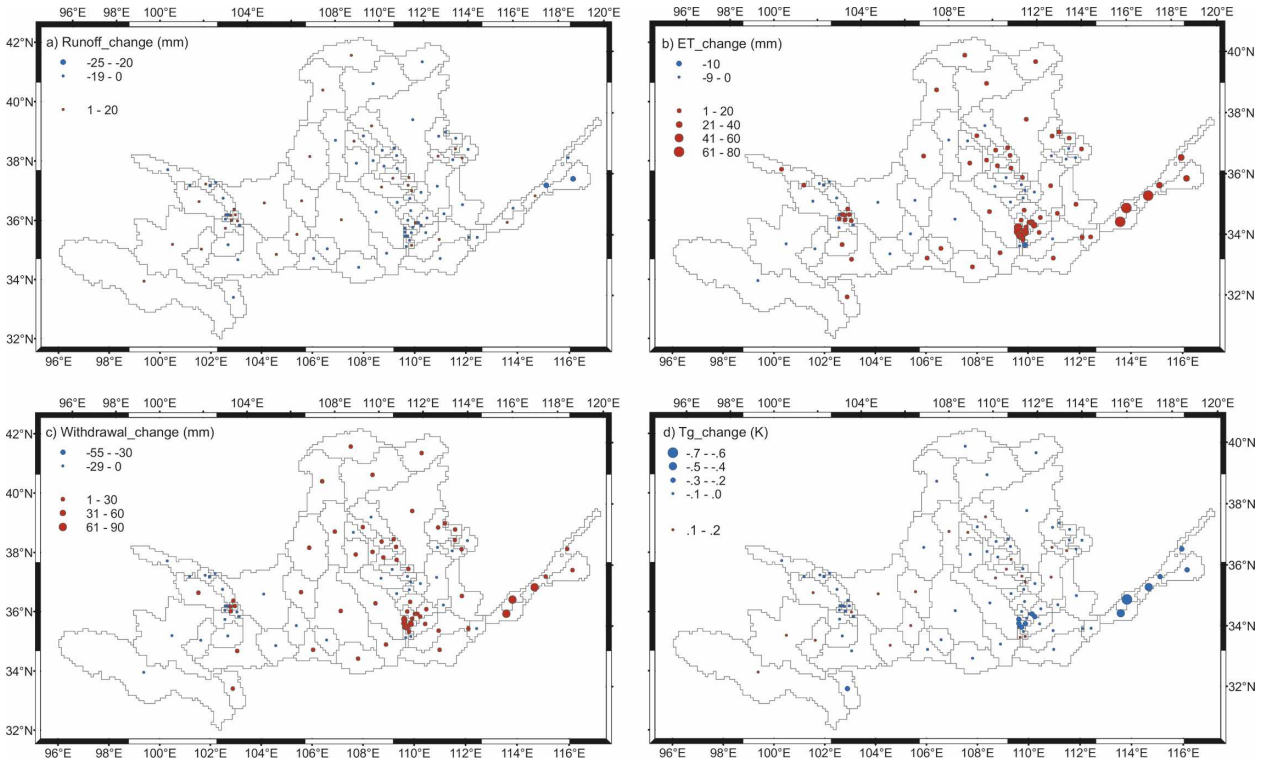

FIG. 11. Same as in Fig. 10 but from vegetation change.

irrigation districts as agriculture develops. Simulated changes in ground surface temperatures are small over much of the basin; however, the ground surface temperature can decrease more than 0.5 K in subbasins with intensive cultivation.

The contributions of irrigation area change to the alteration of the hydrological components in the Yellow River basin from 1960 to 2000 are shown in Fig. 12, which gives the simulated differences between S4 and S1. Generally, runoff increases, evapotranspiration increases, and irrigation water withdrawals increase with spatial patterns that follow the irrigated area increases. Runoff (in which irrigation water withdrawals are not excluded) increases because irrigation return flow increases as irrigation water withdrawals increase. The alterations of hydrological components are small in the upper and middle reaches because of small changes in irrigated area. Larger changes occur in the lower reaches where the irrigated area in the 1990s is more than 5 times of that in the 1960s. However, the change of ground surface temperature is small because the irrigated area alteration is small compared with the area of the entire river basin.

Figure 13 gives the total contributions of changes in climate, vegetation, and irrigated area to the hydrological components (differences between S5 and S1). The climate, vegetation, and irrigated area changes combine to reduce both runoff and evapotranspiration over the Loess Plateau. Comparing Fig. 10 with Fig. 12, the contributions of climate change dominate the runoff and evapotranspiration changes in the Loess Plateau. Runoff and evapotranspiration increase over the Tibetan Plateau and lower reaches of the North China Plain. The increases are contributed by both climate change and human activity. Water withdrawals have increased over the entire river basin. The changes in water withdrawals are mainly caused by the irrigated area increase and the accompanying vegetation condition increase. Climate change over the Loess Plateau leads to increased irrigation water withdrawals. Ground surface temperature increases over most parts of the river basin, primarily as a result of warmer air temperatures. An interesting phenomenon is found in the ground surface temperature in the lower reaches. Water withdrawals for irrigation make the ground temperature decrease while air temperature increases. The effects of the climate change and human activities on ground temperature cancel each other out in the low reaches. Comparing Fig. 13 with Fig. 8, the contribution to runoff decrease from climate linear change, vegetation, and irrigation change is less than the simulated runoff decrease in the control simulation over the Loess Pla-

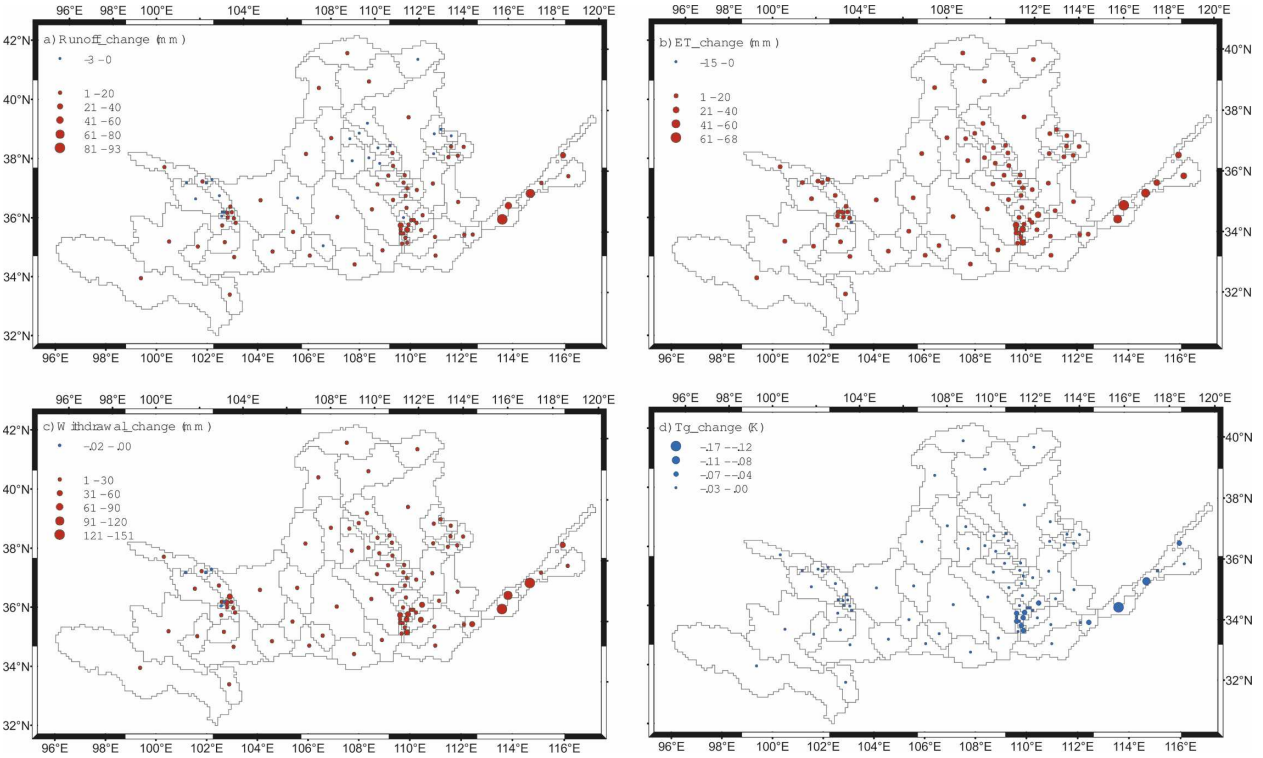

FIG. 12. Same as in Fig. 10 but from irrigation area change.

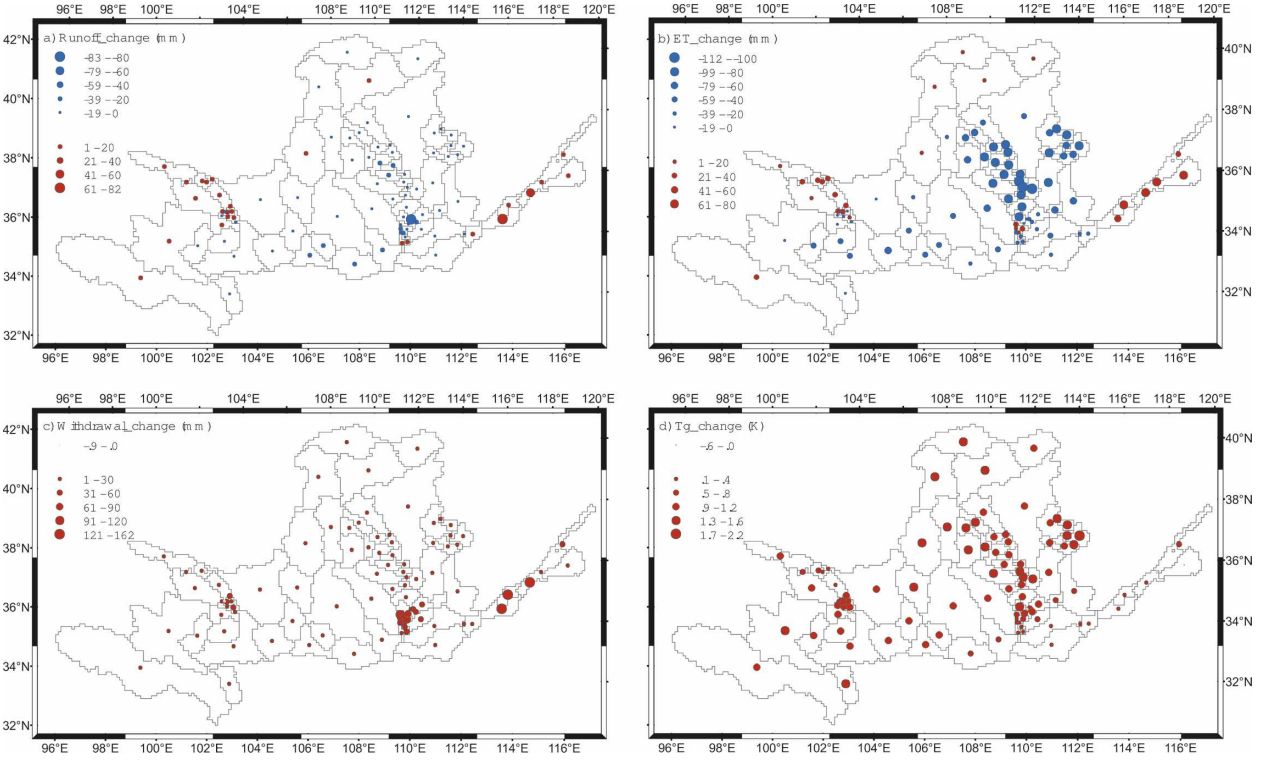

FIG. 13. Same as in Fig. 10 but from climate linear change, vegetation, and irrigation change.

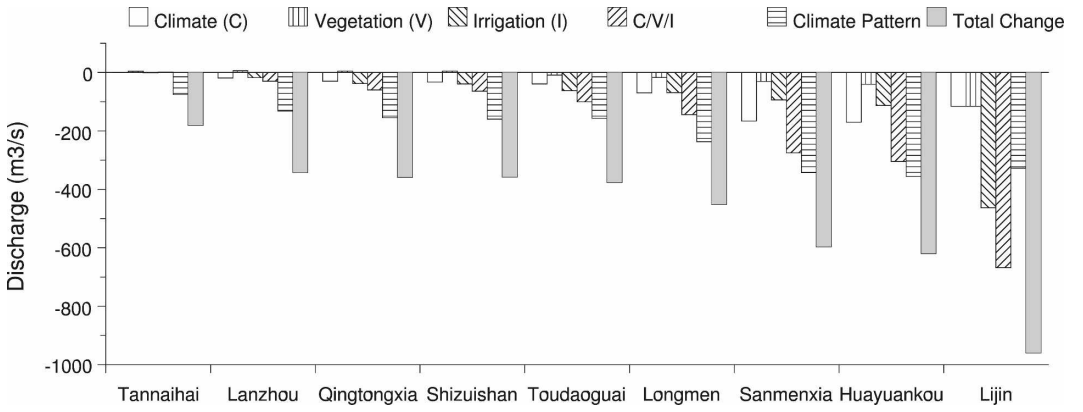

FIG. 14. Contributions of annual discharge change along the river main stem.

teau. The runoff decrease over the Loess Plateau is partly caused by the climate temporal pattern change according to S6.

c. River flow changes

Figure 14 shows the contributions to discharge changes from climate change (C, S2 − S1); vegetation change (V, S3 − S1); irrigation change (I, S4 − S1); C, V, and I (S5 − S1); climate temporal pattern change (S6 − S5); and the total simulated change from control scenario (S1). The sum of contributions from C, V, and I is quite close to that from C, V, and I, implying the climate, vegetation, and irrigation changes independently affect discharge. However, the sum of contributions from C, V, and I and climate temporal pattern change does not fully match the total simulated change because they could be correlated. At the river mouth Lijin station, the control simulation shows a nearly 1000 $m^3 s^{-1}$ decrease during the study period. About 30% of the decrease is caused by the climate temporal pattern change, and 70% is caused by the linear changes in climate, vegetation, and irrigation. Of the 70% caused by linear changes, about 15% is caused by the linear component of climate change, 15% is caused by vegetation change, and 70% is caused by irrigation change. At the Huayuankou station, about half of the discharge decrease is caused by climate temporal pattern change, about one quarter is caused by climate linear change, 5% is caused by vegetation change, and 20% is caused by irrigation change. The different proportion shows the large irrigation change contribution between the Huayuankou and Lijin stations. The result agrees with the large water withdrawals at the Huayuankou-Lijin section to the lower reaches irrigation districts. The vegetation change could be caused by both human activity and climate change. Taking the Huayuankou-Lijin reach, the discharge decrease at Lijin station is mainly caused by irrigation (about 50%), and the discharge decrease caused by direct irrigation is about 40%. Above the Huayuankou station, the discharge change is mainly caused by climate change (about 75%), and the effects of direct irrigation are about 20%. The large linear climate change contribution occurs at the Toudaoguai-Sanmenxia section, where the Loess Plateau responds to precipitation decrease. Large climate temporal pattern contributions are observed for the reach above Lanzhou and the Toudaoguai-Sanmenxia reach, suggesting that not only the linear component of climate change but also the climate temporal pattern has resulted in discharge declines. In addition to the lower reaches, increased irrigation contributions are found in the Tangnaihai-Qingtongxia reach, the Toudaoguai-Shizuishan reach, and the Longmen-Sanmenxia reach, corresponding to the Qingtongxia irrigation district, the Hetao irrigation district, and the Weihe irrigation district, respectively.

The trends in annual hydrological components give an idea of the possible reasons for the Yellow River zero-discharge episodes. Although reservoir operations, which would seem to have considerable potential impact on the terrestrial water cycle, are not considered in this study, and therefore streamflow in the low-flow period would certainly be underestimated (Hanasaki et al. 2006), a high temporal resolution (hourly) simulation provides a surrogate to investigate the incidence of zero-discharge episodes and how they have changed over time. Figure 15 shows the simulated dry days (when the daily mean discharge is less than 10 $m^3 s^{-1}$) and observed zero-discharge days at the river mouth Lijin station. The river flow is assumed to be dry when the discharge is less than minimum flow, 10 $m^3 s^{-1}$. Scenario S1 gave more drying days than observations did. The overestimation of drying days is as expected because of the omission of the reservoir operations,

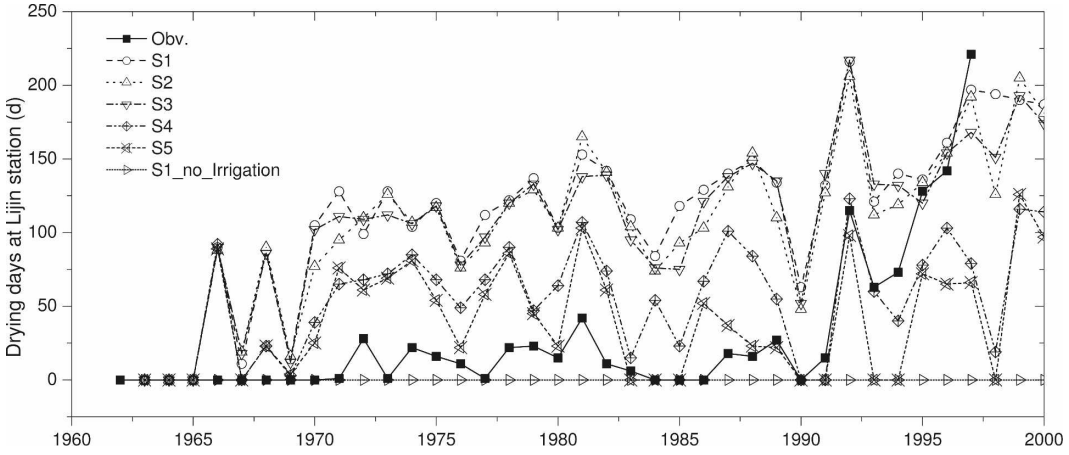

FIG. 15. Simulated and observed drying days at the Lijin station.

although various human decisions on agricultural practices might have an effect. The simulated and observed drying days were close to maximum values during the latter part of the 1990s after several continual dry years. An additional scenario was run based on the S1 scenario without irrigation. The S1 scenario without irrigation gave no zero-discharge days for the entire simulation period, indicating that the Yellow River will not dry in the natural situation without human activities. Scenarios S1–S5 can be partitioned into two groups: the "with irrigation" change group (G1) includes scenarios S1, S2, and S3; and the "without irrigation" change group (G2) includes scenarios S4 and S5. The with irrigation change group shows a rapid increase of drying days, while the without irrigation change group shows modest increases. The difference in zero-discharge days between G1 and G2 became large from the early 1970s, when the irrigated area was rapidly increasing. In G2, the difference in drying days between S4 and S5 became large from the 1980s, implying the contribution to drying days from climate change and vegetation change became large in the 1980s and the 1990s. Even when the irrigated area and climate conditions are kept as in the 1960s, the scenario S5 shows larger drying days than the observations in the 1970s. Because reservoirs are not considered in the simulations, these results imply that the Yellow River would have zero flow at downstream locations without reservoir operations even if the irrigation levels were at the relatively low levels of the 1960s. The reservoirs, which release water for irrigation and also release environmental flows in the low-flow season, make more water available for irrigation on one hand, while at the same time may help to keep environmental flows and counter zero flow. Certainly, there are more sophisticated ways to evaluate streamflow impacts of reservoirs operations. We feel, however, that the scenario analysis results are noteworthy as an index of the practical impact of the reservoir operations.

4. Conclusions and discussion

The DBH model system was used to simulate hydroclimate connections in the Yellow River with the objective of diagnosing possible mechanisms for Yellow River zero-discharge episodes. The results suggest that runoff and evapotranspiration decreases over the Loess Plateau are dominated by climate change during the 1960–2000 study period. Ground temperature increases are predicted over most of the river basin. Irrigation and vegetation change affect some particular parts of the river basin where they induce increased evapotranspiration and water withdrawals. The areas most affected by irrigation and vegetation change are the irrigation districts, especially the Weihe irrigation district and the irrigation districts in the lower reaches. Vegetation recovery in the irrigated areas significantly decreases runoff and cools the ground.

Overall, climate change dominates the predicted changes in the upper and middle reaches, but human activities dominate the lower reaches of the Yellow River basin. Nearly half of the annual river discharge at the river mouth is affected by climate change and half by human activities. The linear trend in climate change contributes to water consumption, but the climate temporal pattern change has a larger impact on annual river discharge than the linear climate change. In the upper and middle reaches, the climate temporal pattern change contributes half of the runoff decrease.

Climate change is the largest contributor to observed changes in the water budget of the upper and middle reaches; however, in the lower reaches river discharge is affected more by irrigation water withdrawals. The

number of zero-flow episodes at the river mouth became large from the early 1970s, when the irrigated area rapidly increased. The contribution to zero-discharge episodes from climate change and vegetation change became large in the 1980s and the 1990s. The results also imply that the Yellow River would have zero flow at the mouth without reservoir operations even if irrigation withdrawals were held to the relatively low level of the 1960s. The reservoirs, which release for irrigation and also release environment flow in the low-flow season, make more water available for irrigation on one hand and may help to maintain environmental flows and counter zero-discharge episodes on the other hand.

Future studies could benefit from a more sophisticated handling of the reservoir system. Implementation of detailed reservoir information could make the reservoir simulation possible and would improve daily streamflow simulation. More sophisticated techniques are also likely to resolve causes of zero-discharge episodes on a finer time scale.

Acknowledgments. The work described in this paper was supported by the JSPS/Grant-in-Aid for Scientific Research, the Ministry of Education, Culture, Sports, Science and Technology (MEXT) of Japan, the Core Research for Evolutional Science and Technology (CREST), the Japan Science and Technology Corporation (JST), and Project 50579031 of the National Natural Science Foundation of China (NSFC). The authors thank Professor Dennis P. Lettenmaier of the University of Washington for his helpful comments and valuable suggestions. Thanks are due to Dr. F. Su for her assistance with the language of the paper.

REFERENCES

Cesaraccio, C., D. Spano, P. Duce, and R. L. Snyder, 2001: An improved model for determining degree-day values from daily temperature data. *Int. J. Biometeor.,* **45,** 161–169.

Chen, J., and X. Mu, 2000: Tendency, causes and control measures on Yellow River dry-up (in Chinese). *J. Nat. Resour.,* **15,** 31–35.

Childs, E. C., 1971: Drainage of groundwater resting on a sloping bed. *Water Resour. Res.,* **7,** 1256–1263.

Chow, V. T., 1959: *Open-Channel Hydraulics.* McGraw-Hill, 680 pp.

Clapp, R. B., and G. M. Hornberger, 1978: Empirical equations for some soil hydraulic properties. *Water Resour. Res.,* **14,** 601–604.

Cosby, B. J., G. M. Hornberger, R. B. Clapp, and T. R. Ginn, 1984: A statistical exploration of the relationships of soil moisture characteristics to the physical properties of soils. *Water Resour. Res.,* **20,** 682–690.

Decharme, B., and H. Douville, 2006: Introduction of a sub-grid hydrology in the ISBA land surface model. *Climate Dyn.,* **26,** 65–78.

FAO, 1995: Digital Soil Map of the World and Derived Soil Properties, version 3.5. Land and Water Digital Media Series 7, Food and Agriculture Organization of the United Nations, CD-ROM.

Feng, J., T. Wang, S. Qi, and G. Xie, 2005: Land degradation in the source region of the Yellow River, northeast Qinghai-Xizang Plateau: Classification and evaluation. *Environ. Geol.,* **47,** 459–466.

Fu, G., S. L. Chen, C. M. Liu, and D. Shepard, 2004: Hydroclimatic trends of the Yellow River basin for the last 50 years. *Climatic Change,* **65,** 149–178.

Haddeland, I., D. P. Lettenmaier, and T. Skaugen, 2006a: Effects of irrigation on the water and energy balances of the Colorado and Mekong river basins. *J. Hydrol.,* **324,** 210–223.

——, T. Skaugen, and D. P. Lettenmaier, 2006b: Anthropogenic impacts on continental surface water fluxes. *Geophys. Res. Lett.,* **33,** L08406, doi:10.1029/2006GL026047.

Hanasaki, N., S. Kanae, and T. Oki, 2006: A reservoir operation scheme for global river routing models. *J. Hydrol.,* **327,** 22–41.

Hirabayashi, Y., S. Kanae, I. Struthers, and T. Oki, 2005: A 100-year (1901–2000) global retrospective estimation of the terrestrial water cycle. *J. Geophys. Res.,* **110,** D19101, doi:10.1029/2004JD005492.

Huang, M., and L. Zhang, 2004: Hydrological responses to conservation practices in a catchment of the Loess Plateau, China. *Hydrol. Processes,* **18,** 1885–1898.

Jiménez, J. I., L. Alados-Arboledas, Y. Castro-Diez, and G. Ballester, 1987: On the estimation of long-wave radiation flux from clear skies. *Theor. Appl. Climatol.,* **38,** 37–42.

Lighthill, M. H., and G. B. Whitham, 1955: On kinematic waves. I. Flood movement in long rivers. *Proc. Roy. Soc. London,* **229,** 281–316.

Liu, C. M., and S. F. Zhang, 2002: Drying up of the Yellow River: Its impacts and counter-measures. *Mitigation Adaptation Strategies Global Change,* **7,** 203–214.

——, and X. Zhang, 2004: Causal analysis on actual water flow reduction in the mainstream of the Yellow River (in Chinese). *Acta Geogr. Sin.,* **59,** 323–330.

——, and H. X. Zheng, 2004: Changes in components of the hydrological cycle in the Yellow River basin during the second half of the 20th century. *Hydrol. Processes,* **18,** 2337–2345.

Liu, L. L., Z. F. Yang, and Z. Y. Shen, 2003: Estimation of water renewal times for the middle and lower sections of the Yellow River. *Hydrol. Processes,* **17,** 1941–1950.

Liu, X. D., and B. D. Chen, 2000: Climatic warming in the Tibetan Plateau during recent decades. *Int. J. Climatol.,* **20,** 1729–1742.

Loveland, T. R., B. C. Reed, J. F. Brown, D. O. Ohlen, Z. Zhu, L. Yang, and J. W. Merchant, 2000: Development of a global land cover characteristics database and IGBP DISCover from 1 km AVHRR data. *Int. J. Remote Sens.,* **21,** 1303–1330.

Ministry of Water Resources, 1991: *Almanac of China Water Resources 1990 (Zhongguo Shuili Nianjian 1990)* (in Chinese). China Waterpower Press, 723 pp.

Mo, X. G., S. X. Liu, Z. H. Lin, and W. M. Zhao, 2004: Simulating temporal and spatial variation of evapotranspiration over the Lushi basin. *J. Hydrol.,* **285,** 125–142.

Myneni, R. B., R. R. Nemani, and S. W. Running, 1997: Estimation of global leaf area index and absorbed par using radia-

tive transfer models. *IEEE Trans. Geosci. Remote Sens.,* **35,** 1380–1393.

Nash, J. E., and J. V. Sutcliffe, 1970: River flow forecasting through conceptual models. Part I–A discussion of principles. *J. Hydrol.,* **10,** 282–290.

Nijssen, B., G. M. O'Donnell, D. P. Lettenmaier, D. Lohmann, and E. F. Wood, 2001: Predicting the discharge of global rivers. *J. Climate,* **14,** 3307–3323.

Oki, T., and S. Kanae, 2006: Global hydrological cycles and world water resources. *Science,* **313,** 1068–1072.

——, T. Nishimura, and P. Dirmeyer, 1999: Assessment of annual runoff from land surface models using Total Runoff Integrating Pathways (TRIP). *J. Meteor. Soc. Japan,* **77,** 235–255.

Revfeim, K. J. A., 1997: On the relationship between radiation and mean daily sunshine. *Agric. For. Meteor.,* **86,** 181–191.

Russell, G. L., and J. R. Miller, 1990: Global river runoff calculated from a global atmospheric general circulation model. *J. Hydrol.,* **117,** 241–254.

Sellers, P. J., and Coauthors, 1996: A revised land surface parameterization (SiB2) for atmospheric GCMs. Part I: Model formulation. *J. Climate,* **9,** 676–705.

Sheffield, J., G. Goteti, F. Wen, and E. F. Wood, 2004: A simulated soil moisture based drought analysis for the United States. *J. Geophys. Res.,* **109,** D24108, doi:10.1029/2004JD005182.

Siebert, S., P. Döll, S. Feick, and J. Hoogeveen, 2005: Global Map of irrigated areas version 3.0. Johann Wolfgang Goethe Universität, Frankfurt am Main, Germany, and Food and Agriculture Organization of the United Nations, Rome, Italy. [Available online at http://www.fao.org/nr/water/aquastat/irrigationmap/index.stm.]

Sun, R., C. M. Liu, and Q. Zhu, 2001: Relationship between the fractional vegetation cover change and rainfall in the Yellow River Basin (in Chinese). *Acta Geogr. Sin.,* **56,** 667–672.

Tang, Q., 2006: A distributed biosphere-hydrological model for continental scale river basins. Ph.D. thesis, University of Tokyo, 181 pp.

——, T. Oki, and S. Kanae, 2006: A distributed biosphere hydrological model (DBHM) for large river basin. *Ann. J. Hydraul. Eng. JSCE,* **50,** 37–42.

——, H. Hu, and T. Oki, 2007a: Groundwater recharge and discharge in a hyperarid alluvial plain (Akesu, Taklimakan Desert, China). *Hydrol. Processes,* **21,** 1345–1353.

——, T. Oki, S. Kanae, and H. Hu, 2007b: A spatial analysis of hydro-climatic and vegetation condition trends in the Yellow River basin. *Hydrol. Processes,* **22,** 451–458.

——, ——, ——, and ——, 2007c: The influence of precipitation variability and partial irrigation within grid cells on a hydrological simulation. *J. Hydrometeor.,* **8,** 499–512.

Towner, G. D., 1975: Drainage of groundwater resting on a sloping bed with uniform rainfall. *Water Resour. Res.,* **11,** 144–147.

Vitousek, P. M., H. A. Mooney, J. Lubchenco, and J. M. Melillo, 1997: Human domination of Earth's ecosystems. *Science,* **277,** 494–499.

Wang, G., J. Qian, G. Cheng, and Y. Lai, 2001: Eco-environmental degradation and causal analysis in the source region of the Yellow River. *Environ. Geol.,* **40,** 884–890.

Xia, J., Z. G. Wang, G. S. Wang, and G. Tan, 2004: The renewability of water resources and its quantification in the Yellow River basin, China. *Hydrol. Processes,* **18,** 2327–2336.

Xu, J. X., 2005a: Temporal variation of river flow renewability in the middle Yellow River and the influencing factors. *Hydrol. Processes,* **19,** 1871–1882.

——, 2005b: The water fluxes of the Yellow River to the sea in the past 50 years, in response to climate change and human activities. *Hydrol. Processes,* **35,** 620–631.

Yang, D., C. Li, H. Hu, Z. Lei, S. Yang, T. Kusuda, T. Koike, and K. Musiake, 2004a: Analysis of water resources variability in the Yellow River of China during the last half century using historical data. *Water Resour. Res.,* **40,** W06502, doi:10.1029/2003WR002763.

——, ——, G. Ni, and H. Hu, 2004b: Application of a distributed hydrological model to the Yellow River basin (in Chinese). *Acta Geogr. Sin.,* **59,** 143–154.

Yang, K., and T. Koike, 2005: A general model to estimate hourly and daily solar radiation for hydrological studies. *Water Resour. Res.,* **41,** W10403, doi:10.1029/2005WR003976.

——, G. W. Huang, and N. Tamai, 2001: A hybrid model for estimating global solar radiation. *Sol. Energy,* **70,** 13–22.

Yang, S., C. Liu, and R. Sun, 2002: The vegetation cover over last 20 years in Yellow River Basin (in Chinese). *Acta Geogr. Sin.,* **57,** 679–684.

Yellow River Commission, 1999: Some basic data of the Yellow River (in Chinese). *The Yellow River Newspaper (Huanghe bao),* 1 October, 888.